LWT - Food Science and Technology 50 (2013) 531–537

Contents lists available at SciVerse ScienceDirect

LWT - Food Science and Technology

journal homepage: www.elsevier.com/locate/lwt

Quinoa protein–chitosan–sunflower oil edible film: Mechanical, barrier and structural properties

Carolina Valenzuela, Lilian Abugoch*, Cristian Tapia

Departamento de Ciencia de los Alimentos y Tecnología Química, Facultad de Ciencias Químicas y Farmacéuticas, Universidad de Chile, Vicuña Mackenna 20, Providencia, Santiago, Chile

ARTICLE INFO

Article history:
Received 2 May 2012
Received in revised form
7 August 2012
Accepted 16 August 2012

Keywords:
Quinoa protein
Chitosan
Sunflower oil
Edible films

ABSTRACT

Quinoa protein extracts (Q) were prepared and alkalised at pH 8 and 12 (Q-8 and Q-12). Qs were mixed with chitosan (CH) to form Q/CH mixtures. The optimal proportion of the mixtures was determined by the formation of coacervates. All the films were obtained by solution casting. From the optimal Q/CH mixture and the addition of three different concentrations of sunflower oil (SO) 2.9, 3.8 and 4.7 g/100 mL, and the optimal proportion of SO g/100 mL was selected based on the mechanical and barrier properties of the films. The CH, Q/CH and Q/CH/SO optimal blend films were characterised by FTIR, X-ray diffraction, and SEM. The physicochemical properties of the films were also evaluated. The 0.1 Q-8/CH blend was selected due to its high degree of interaction between the quinoa proteins and CH. The optimum concentration of SO used in the Q-8/CH/SO film was 2.9 g/100 mL. The addition of SO to the film improved the water-vapour permeability (WVP) as a result of hydrophobic interactions and the presence of clusters of hydrophobic masses on the surfaces of these films but reduced the film's tensile strength and oxygen permeability due to the formation of micropores and microfractures detected by SEM.

1. Introduction

Hydrocolloids such as polysaccharides and proteins and their mixtures have been extensively studied for the preparation of edible films (Falguera, Quintero, Jiménez, Muñoz, & Ibarz, 2011; Krochta, 2002; Nisperos-Carriedo, 1994). However, their application is limited by the high water-vapour permeability (WVP) that these films exhibit due to their hydrophilic nature (McHugh & Krochta, 1994; Phan The, Debeaufort, Voilley, & Luu, 2009) and by the need to use plasticising agents to obtain stretchable films (Kowalczyk & Baraniak, 2011; McHugh, Aujard, & Krochta, 1994). This is a significant drawback because the effective control of moisture transfer is a desirable property for most foods. To improve the water-barrier properties of hydrocolloid-based films, lipid compounds are frequently incorporated into these structures (Morillon, Debeaufort, Blond, Capelle, & Voilley, 2002; Vargas, Albors, Chiralt, & González, 2009), causing a decrease in the WVP values at the expense of a reduction in the tensile strength and elasticity of the composite films (Khwaldia, Banon, Desobry, & Hardy, 2004; Srinivasa, Rameshb, & Tharanathana, 2007; Vargas et al., 2009; Zahedi, Ghanbarzadeh, & Sedaghat, 2010); this negatively impacts the applicability of the emulsified films, which is also affected by sensorial alterations that have been shown to characterise foods coated with composite films featuring high amounts of lipids such as saturated acids and waxes (Perez-Gago, Rojas, & Del Rio, 2002; Tanada-Palmu & Grosso, 2005). Nevertheless, some authors have reported composite films featuring unsaturated oils rich in oleic acid that can potentially improve the moisture-barrier properties of hydrophilic films, preventing drastic changes in the mechanical properties of the emulsified films, as these are liquid at room temperature, and hence are easily miscible with biopolymers (Ghanbarzadeh & Almasi, 2011; Ham-Pichavant, Sèbe, Pardon, & Coma, 2005; Muzzarelli, Frega, Miliani, Muzzarelli, & Cartolari, 2000). When hydrocolloid and lipid ingredients are combined, they may interact favourably, resulting in edible films with improved structural and functional properties, as the mechanical and barrier properties depend not only on the compounds used in the polymer matrix but also on their compatibility (Altenhofen, Krause, & Guenter, 2009). Moreover, the study published by Abugoch, Tapia, Villamán, Yazdani-Pedram, and Díaz-Dosque (2011) reported that by blending quinoa protein extracted at alkaline pH and chitosan, an edible film was created without using a plasticiser; this film showed extremely high elongation at break. However, the presence of quinoa proteins resulted in increased WVP. Therefore, the addition of a hydrophobic agent such as sunflower oil in small proportions could improve these films'

* Corresponding author. Tel.: +56 2 9781635; fax: +56 2 2227900.
E-mail addresses: labugoch@uchile.cl, liligoch@gmail.com (L. Abugoch).

0023-6438/$ – see front matter © 2012 Elsevier Ltd. All rights reserved.
http://dx.doi.org/10.1016/j.lwt.2012.08.010

barrier properties against water vapour, which would slightly affect the films' mechanical properties due to the higher elongation relative to that of quinoa proteins conferred to the edible blend films. The aim of this work was to prepare and characterise edible blend films based on quinoa protein, chitosan and sunflower oil, which show good mechanical and water-vapour-barrier properties.

2. Material and methods

2.1. Material

Quinoa flour (*Chenopodium quinoa* Willd.) was supplied by "Cooperativa Las Nieves", VI Region of Chile. The flour was stored at 4 °C until use. The chemical composition of the quinoa flour on a dry basis (db) was as follows: moisture (10.7 ± 0.2 g/100 g db), protein (14.4 ± 0.2 g/100 g db), fat (8.4 ± 0.1 g/100 g db), ash (2.5 ± 0.1 g/100 g db) and carbohydrate (66.1 g/100 g db by difference). Chitosan (CH) was obtained from crab shells (Sigma–Aldrich, USA) with a deacetylation degree of 75–80% and a viscosity of 989.1 ± 26.2 and 640.5 ± 35.7 cP at 2 g/100 mL and 1.5 g/100 mL in citric acid 0.1 mol/L solution, respectively. Sunflower oil (SO) (≥70 g/100 g oleic acid) was purchased from Camilo Ferrón Chile S.A. Tween 80 (T_{80}) was purchased from Comercial Montero Chile Ltda.

2.2. Preparation of aqueous quinoa protein extracts (Q)

The quinoa flour was suspended in distilled water (18 g/100 mL), and the pH was adjusted to pH 8 and 12 with 1 mol/L NaOH. These suspensions were stirred for 60 min at room temperature and centrifuged at 21,000 × *g* for 30 min at 15 °C. The supernatants obtained at pH 8 and pH 12 were denominated aqueous quinoa protein extracts Q-8 and Q-12, respectively. The soluble protein contents of Q-8 and Q-12 were measured according to the Bradford method (Bradford, 1976) and were expressed as mg of protein/mL. The Qs were prepared and used immediately every time it was required.

2.3. Preparation chitosan solutions (CH)

Solutions composed of 1.5 and 2 g/100 mL of CH in citric acid 0.1 mol/L were prepared. The solutions were sonicated for 30 min (Fisher Scientific FS30H, Germany) and left overnight at 4 °C to eliminate bubbles.

2.4. Preparation of quinoa protein extracts–chitosan blends (Q/CH) and determination of the optimal Q/CH ratio

The blends were prepared by mixing solutions of Q-8 or Q-12 and CH (2 g/100 mL) with different Q/CH ratios (0.1, 0.2 and 0.4) using a blade homogeniser (Bosch MSM6A3R 750w, China). The pH of the mixtures was adjusted to 3.0 with 1 mol/L citric acid, and stirring was continued for 30 min. The mixtures were centrifuged at 21,000 × *g* for 20 min at 25 °C. The supernatant viscosity of the blends Q/CH was measured at 25 ± 0.1 °C using a Cannon-Fenske viscometer N°100 (Tapia et al., 2002), and the supernatant soluble protein content of the blends Q/CH was measured using the Bradford method (Bradford, 1976).

2.5. Preparation of quinoa protein extracts–chitosan–sunflower oil blends (Q/CH/SO)

The optimal Q/CH ratio was blended with SO at different concentrations (2.9, 3.8 and 4.9 g/100 mL) and T_{80} (0.6, 0.8 and 1.0 g/100 mL). The blends were prepared by mixing Q, SO and T_{80} at room temperature for 10 min and were homogenised with a high-speed Ultraturrax (Silverson L4R Machines, United Kingdom) for 10 min at 10,000 rpm. Then, CH (2% g/100 mL) was incorporated into the blend by mixing with a blade homogeniser (Bosch MSM6A3R 750w, China) for 10 min at 1000 rpm. The pH was adjusted to 3.0 with citric acid. Film-forming CH/Q/SO blends were sonicated for 30 min (Fisher Scientific FS30H Germany) to eliminate bubbles.

2.6. Film preparation

The optimal Q/CH ratio, Q/CH/SO blends and CH at 1.5 g/100 mL (as control) (37 mL) were cast on a horizontal surface in low-density polyethylene boxes (diameter = 14 cm). The Q/CH and CH films were dried to a constant weight at 50 °C (≈7 h) and Q/CH/SO at 35 °C (≈9 h). The dried films were removed carefully from the boxes and conditioned in an environmental chamber (Model LTH-0150E, Labtech, Co., Korea) at 23 °C and 60% relative humidity for 48 h before being used.

2.7. Functional characterisation of films

2.7.1. Thickness

The thickness (mm) of five samples of each film was determined, averaging the measurements taken at nine points on each film using a digital micrometer (Mitutoyo 293340, Japan).

2.7.2. Mechanical properties

The tensile properties of the films (tensile strength, TS, and per cent elongation at break, %*E*) were determined using the Official Chilean Standard Method (NCh1151, 1999), equivalent to the ISO R1184-1970 standard method, on a universal tensile testing machine (LLOYD, Model LR5K, England) operated with a 5 kN load cell and controlled by DAPMAT version 3.0 software. Five film samples were cut into 10 mm × 50 mm strips and were tested using a double clamp with a separation of 30 mm at a test speed of 20 mm/min. The TS and %*E* values reported are the averages of at least five measurements performed for each type of film. The TS was expressed in MPa and was calculated according to Equation (1):

$$TS = N/mm^2 \quad (1)$$

where

TS is the tensile strength in MPa
N is the force maximum at rupture of the film
mm^2 is the initial cross-sectional area of the film.
The *E*% was calculated according to Equation (2):

$$E\% = \frac{\left(D_f - D_i\right)}{D_i} \times 100 \quad (2)$$

where

E% is the per cent elongation at break
D_f is the distance elongation at break (mm)
D_i is the initial distance between the baselines (mm).

2.7.3. Water-vapour permeability (WVP)

The moisture content (MC) was determined by method 945.15 (AOAC, 1996). The WVP measurements were performed according to the Official Chilean Standard Method (NCh2098, 2000), equivalent to the ASTM D1653-93 and DIN 52615 standard methods, using the wet cup method. A cup was filled with distilled water to a height of 6 mm from the top edge. The film was adhered to the cup with silicone gel,

and the cup was placed in an environmental chamber (Model LTH-0150E, Labtech, Co., Korea) at 23 °C and 60% RH. The weight of the cup was measured daily over 21 days. The WVP values reported are the averages of six measurements performed for each type of film. The WVP was estimated using Equation (3):

$$\mathrm{WVP} = \frac{\Delta m}{tA\Delta P} \times \varepsilon \quad (3)$$

Where:

WVP is the water-vapour permeability in g mm/m^2 d kPa.
Δm is the mass change over time in g. t is the time in days
A is the film area in m^2.
ΔP is the partial vapour pressure difference of the atmosphere and pure water (112.353 kPa at 23 °C).
ε is the thickness in mm.

2.7.4. Oxygen permeability (OP)

The oxygen permeability (OP) of the fully formed films (diameter = 14 cm) was determined using an OX-TRAN system (MS-2/20, Mocon Inc., USA) coupled with a coulometric sensor at 23 °C and 0% RH, according to the ASTM DIN-3935 procedure (ASTM, 1981). Films samples were conditioned in an environmental chamber (Model LTH-0150E, Labtech, Co., Korea) at 23 °C and 60% RH for 48 h prior to testing, then placed between 2 aluminium masks with a circular area of 50 mm^2.

2.8. Structural characterisation of films

Structural analysis was carried out on the optimal Q/CH and Q/CH/SO ratio films and CH film.

2.8.1. X-ray diffraction (XRD)

X-ray diffraction measurements were performed on a Siemens D-5000 powder X-ray diffractometer with CuKα radiation (λ 1.54 Å); a 0.02° step and 2θ range of 1.7–80° were selected to analyse the crystal structure.

2.8.2. Fourier transform infrared spectroscopy (FTIR)

Complete films (diameter = 14 cm) were placed on the horizontal attenuated reflectance accessory, made of ZnSe, of a Spectrum® Fourier transform infrared spectrometer (Perkin Elmer, Model 400, Beaconsfield, United Kingdom). Spectra were obtained by averaging 20 scans over the spectral range of 650–4000 cm^{-1}.

2.8.3. Film microstructure

The microstructure of the films was characterised by scanning electron microscopy (SEM) on a LEO Scanning Electron Microscope operating at 25 kV (SEM; LEO 1420 VP, Cambridge, UK). Prior to examination, the samples were then mounted on a cylindrical aluminium stub, cut like a straight chair, upon which the films were fixed using a double-sided tape, which was applied to allow for the observation of the films' surface morphology. The films were then gold-sputter-coated for 3 min at 20 kV in an argon atmosphere (PELCO 91000) to render them electrically conductive.

2.9. Physicochemical characterisation of films

2.9.1. Water activity (a_w)

The a_w of the films was measured at 25 °C by the graphic interpolation method (Prior, 1979).

2.9.2. Colour

The colour of the film samples was measured with a colourimeter (Hunter Lab system, Model Miniscan 2.0/45, USA) using the Hunter Lab colour scale. These parameters were used to calculate the chroma (Equation (4)) and hue angle (Equation (5)). The films were cuts into pieces measuring approximately 40 mm in a die to fit the size of the cylindrical container specially designed for the colourimeter and placed on the bottom of the container.

Chroma:

$$\mathrm{Chroma} = (a^*2 + b^*2)^{1/2} \quad (4)$$

Hue angle:

$$\mathrm{Hue} = \tan^{-1}(b^*/a^*) \quad (5)$$

where a^* and b^* = Hunter Lab parameters.

2.10. Statistical analysis

Statgraphics plus 5 was used for all of the statistical analyses. Analysis of variance (ANOVA) and significance of differences between the means of Tukey's multiple range tests at a p level of 0.05 were used to determine significance.

3. Results and discussion

3.1. Optimal Q/CH blend ratio

Fig. 1 shows how the relative viscosity (V) and soluble protein (SP) supernatant changed when the extraction pH of the quinoa protein extract (Q) and Q/CH ratio were changed. The optimal ratio between the polymers occurs when the V and SP supernatant content is minimum, which means that both polymers react completely to form a coacervate (Tapia et al., 2002). This optimal ratio was dependent on the pH extraction of quinoa protein and on the Q/CH ratio used in the mixtures. It was observed that the blends between Q-8 and CH formed coacervate complexes with a high degree of interaction. The region of the curve where there is a low amount of supernatant SP and V in the mixtures was the 0.1 Q-8/CH because, in this region, the ionisable groups of both components, such as the protonated groups of CH and the anionic groups of quinoa proteins, could be balanced, forming the complex by electrostatic attraction.

On the other hand, the interaction between Q-12 and CH showed a high amount of V and SP supernatant, these increased at

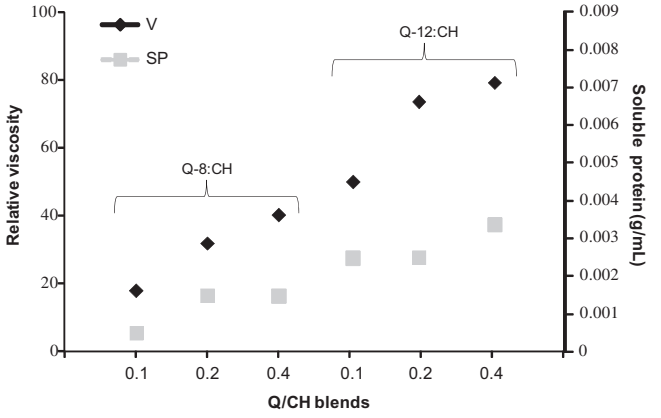

Fig. 1. Relative viscosity (V) and soluble protein content (SP) in supernatant of quinoa protein extracted (Q) at pH 8 and 12/chitosan (CH) blends (Q-8 or 12/CH).

higher protein concentrations (Fig. 1). This phenomenon is possibly related to the high pH obtained by these mixtures near the pKa of CH = 6.0–6.3 (Kumar, Muzzarelli, Muzzarelli, Sashiwa, & Domb, 2004), which could lead to a lower ionisation of CH and consequently a reduced Q-12/CH interaction. Additionally, the high pH used for the extraction of Q-12 may have caused the denaturation of the quinoa proteins, altering their ability to interact with the CH. Therefore, the optimal blend was 0.1 Q-8/CH.

3.2. Optimal Q/CH/SO blend film

3.2.1. Mechanical properties

Table 1 shows the thickness (*T*), tensile strength (TS), and percentage elongation at break (*E*%) of the films. The films thickness ranged from 32 to 126 μm, and these values increased significantly ($p < 0.05$) as more components were added to the CH films because the film thickness depended on the film's nature and composition (Sebti, Chollet, Degraeve, Noel, & Peyrol, 2007); the thickness increased especially with the incorporation of hydrophobic molecules (Ghasemlou, Khodaiyan, Oromiehie, & Saeid-Yarmand, 2011; Phan The et al., 2009).

The TS values of the Q-8/CH film (2.7 MPa) and Q-8/CH/SO films (0.99–0.56 MPa) were significantly lower than those of the CH films (13.4 MPa) ($p < 0.05$). The TS of the CH films decreased when quinoa proteins were incorporated into the CH matrix, as reported by Abugoch et al. (2011). The incorporation of SO into the Q-8/CH/SO matrix caused a decrease in TS values, which was indirectly proportional to the SO concentration added. Other authors have also observed a decrease in TS values by adding lipids to the hydrocolloid matrix (Bonilla, Atarés, Vargas, & Chiralt, 2012; Ghasemlou et al., 2011; Vargas et al., 2009). This effect could be attributed to the heterogeneity introduced in the film structure and the negative effect on the cohesion forces of the Q-8/CH matrix by SO incorporation (Perez-Gago & Krochta, 2001; Petersson & Stading, 2005).

The mean %*E* values (Table 1) show that the presence of quinoa protein in Q-8/CH films (178%) increased the extensibility by up to 9 times relative to the extensibility of the CH film (21%), indicating a plasticising effect caused by quinoa protein, as described by Abugoch et al. (2011). The addition of SO to Q-8/CH/SO blend films generated a lubricating effect, increasing the extensibility of these films from 55 to 136%, which was significantly higher in the Q-8/CH/2.9SO films ($p < 0.05$), and decreasing the extensibility with higher SO concentrations. Some researchers have reported that the addition of lipids to edible films enhances the films' *E*% (Bertan, Tanada-Palmu, Siani, & Grosso, 2005; Pereda, Amica, & Marcovich, 2012). However, many studies have reported the opposite effect (Guerrero, Hanani, Kerry, & Caba, 2011; Péaroval, Debeaufort, Despera, & Voilley, 2002). Compared to the *E*% values of other emulsified edible films, such as chitosan/1 g/100 mL to 4 g/100 mL oleic acid (*E*% = 11–15%) (Vargas et al., 2009), chitosan/5–15 g/100 mL olive oil (*E*% = 22–33%) (Pereda et al., 2012), and soy protein isolate/glycerol/5–15 g/100 g oleic acid (*E*% = 19–23%) (Guerrero et al., 2011), Q-8/CH/2.9SO blend films had higher *E*% values, although these films have been formed without plasticisers.

3.2.2. Barrier properties

Table 1 shows the moisture content (MC) and water-vapour permeability (WVP) of the films. The MC was significantly higher for the Q-8/CH and CH films than the Q-8/CH/SO films ($p < 0.05$). For the Q-8/CH/SO blend films, a significant decrease in MC% ($p < 0.05$) was observed when a greater amount of SO was incorporated into the films. This is attributed to the fewer sites available for water sorption in the polymeric matrix due to the increase in the number of hydrophobic chains.

The WVP values were significantly lower for all Q-8/CH/SO blend films compared with the Q-8/CH and CH films ($p < 0.05$) due to the non-polar character of the SO component. The results show that the presence of SO reduced the WVP values by 30% relative to the values of the hydrocolloid. The lower WVP values obtained with SO addition can be explained by the formation of an interconnecting lipid network within the film matrix, which provides hydrophobicity and thus reduces the adsorption of water molecules, as has been observed in emulsified films by other authors (Fabra, Pérez-Masiá, Talens, & Chiralt, 2011; Shellhammer & Krochta, 1997). This is consistent with the low TS values of these films, which are possibly due to the effect of greater SO concentrations on the cohesion forces of the polymer network being predominant over hydrophobic effects; thus, water-vapour transport is greater in disrupted films. Moreover, it is reported that the incorporation of a higher amount of hydrophobic material into an emulsion film does not guarantee reduced WVP because the permeability of emulsion films is influenced by the steric hindrance and "tortuosity" of the diffusion of water molecules (Cheng, Abd Karim, & Seow, 2008) and by the existence of pores, voids, cracks and channels through the matrix (Wong, Gastineau, Gregorski, Tillin, & Pavlath, 1992).

Comparing the WVP values of Q-8/CH/SO films (0.277–0.289 g mm/m^2 d kPa) with those of other biopolymeric films shows that they are similar to those of emulsified films of chitosan with higher olive oil concentrations of 5–15 g/100 mL (0.286–0.325 g mm/m^2 d kPa) (Pereda et al., 2012) but lower than those of other edible films such as pistachio globulin/2–6 g/100 g palmitic or stearic acid (55–61 g mm/m^2 d kPa) (Zahedi et al., 2010), soy protein isolate plus oleic acid and beeswax (4–5 g mm/m^2 d kPa) (Monedero, Fabra, Talens, & Chiralt, 2009).

Table 1 shows the oxygen permeability (OP) values of the films. The CH film exhibited excellent oxygen-barrier properties (<0.1 cm^3 μm/m^2 d kPa), as has been observed by other authors (Park, Marsh, & Rhim, 2002). These OP values are significantly lower than those of the Q-8/CH film (24.1 ± 4.3 cm^3 μm/m^2 d kPa) and Q-8/CH/SO films (92.4–149.6 cm^3 μm/m^2 d kPa) ($p < 0.05$). The

Table 1
Thickness (*T*), tensile strength (TS), elongation at break (*E*), moisture content (MC), water-vapour permeability (WVP) and oxygen permeability (OP) of chitosan film (CH), quinoa protein extract at pH 8/chitosan blend film (Q-8/CH) and quinoa protein extract at pH 8/chitosan/sunflower oil blends films (Q-8/CH/SO).

Edible films	Properties					
	T (μm)	TS (MPa)	*E* (%)	MC (%)	WVP[a]	OP[b]
CH	32 ± 2^A	13.4 ± 1.1^A	20.7 ± 4.3^A	10.9 ± 1.0^A	0.403 ± 0.016^A	>0.1^A
Q-8/CH	51 ± 1^B	2.7 ± 0.4^B	177.8 ± 25.9^B	10.7 ± 0.5^A	0.397 ± 0.018^A	24.1 ± 4.3^B
Q-8/CH/2.9SO	101 ± 9^C	0.99 ± 0.1^C	136.4 ± 10.7^C	9.2 ± 0.4^B	0.289 ± 0.011^B	92.4 ± 10.4^C
Q-8/CH/3.8SO	111 ± 10^C	0.78 ± 0.2^D	97.3 ± 8.1^D	8.7 ± 0.3^C	0.281 ± 0.011^B	128.1 ± 11.2^D
Q-8/CH/4.7SO	126 ± 8^D	0.56 ± 0.1^E	55.1 ± 8.9^E	8.1 ± 0.3^D	0.277 ± 0.009^B	149.6 ± 16.0^E

Mean values in the same column with different letters differ significantly ($p < 0.05$).
[a] WVP (g mm/m^2 d kPa).
[b] OP (cm^3 μm/m^2 d kPa).

addition of quinoa protein to the Q-8/CH films produced more than a two-hundred-fold increase in the OP of the CH films due to new interactions that are generated in the network between quinoa protein and chitosan, which can disorder the structure. The OP values increased drastically with the addition of SO. Adding SO also increased the gas oxygen permeation up to 920–1500 times, probably due to a significant decrease in the crystalline spacing by matrix restructuring after the addition of lipids molecules, which generate channel sand pores in the network; this facilitates O_2 diffusion (Bertan, Fakhouri, Siani, & Grosso, 2005; Kester & Fennema, 1989) because the OP of edible films is attributable to capillary mechanisms (Morillon et al., 2002).

Finally, the Q-8/CH/2.9SO blend film was chosen due to its good mechanical behaviour and its lower WVP relative to the hydrophilic films (Q-8/CH and CH).

Because the gas and WVP of edible films and coatings depend on several factors, such as the integrity of the film, the ratio between crystalline and amorphous zones, the hydrophilic-hydrophobic ratio and the polymeric chain mobility (García, Martino, & Zaritzky, 2000), it is expected that an analysis of the structural properties of these films contributes to an understanding of the changes in the films' mechanical and permeability properties.

3.3. Structural characterisation of films

3.3.1. Film X-ray diffraction

Fig. 2 shows the XRD patterns of the edible films. The diffractogram of the CH film shows partially crystalline nature, presenting a strong and sharp diffraction peak at 2θ 19.3°, which is the typical fingerprint for chitosan films (Zhong, Songa, & Li, 2011).

The diffraction patterns of the Q-8/CH blend films (Fig. 2) show sharp and well-defined characteristic peaks at 2θ 19.3°, 35.9°, 39.6°, 43.4°, 47.3° and 48.9°, suggesting the existence of intermolecular interactions between both polymers, which means that there is good compatibility between CH and quinoa protein, as demonstrated by Abugoch et al. (2011).

The intensity of the diffraction-pattern peaks of the Q-8/CH/2.9SO blend films (Fig. 2) were less intense, flatter and broader, indicating that the introduction of SO into the film matrix generated a less crystalline structure, which could be attributed to the fact that the intermolecular interactions among the components of the composite network limited the movements of the molecular chain segments and restrained the crystallisation process. However, the incorporation of SO improves the miscibility of the components.

3.3.2. Fourier transform infrared spectroscopy (FTIR)

Fig. 3 shows the FTIR spectra of the CH, Q-8/CH and Q-8/CH/2.9SO films. The main absorption peaks between 3500 and 3200 cm^{-1} in the spectra of the CH and Q-8/CH films are indicative of the O–H vibration; these groups are able to form hydrogen bonds by the electrostatic interaction between the cationic groups of CH and the anionic groups of quinoa protein (Abugoch et al., 2011). The FTIR spectrum of the Q-8/CH/2.9SO film shows less absorption at 3263 cm^{-1}, indicating reduced ionic interaction compared with hydrocolloid-based films. The peak at 3004 cm^{-1}, which was observed exclusively in the FTIR spectrum of the Q-8/CH/2.9SO film, corresponded with the *cis* conjugated unsaturations of oleic acid (Muik, Lendl, Molina-Díaz, & Ayora-Cañada, 2005), the main component of SO. The main absorption peaks of the Q-8/CH/2.9SO film occurred at 2853–2701 cm^{-1} (C–H stretching), which are associated with hydrophobic interactions. These absorption bands have been reported for other emulsified films (Andreuccetti, Carvalho, & Grosso, 2010; Pereda, Aranguren, & Marcovich, 2010). In contrast, the FTIR spectrum of the CH and Q-8/CH films showed negligible absorption in this zone due to the hydrophilic characteristics of both compounds. The peak at 1737–1731 cm^{-1}, common to all films, corresponded to the carbonyl group (C=O). This band was higher for Q-8/CH/2.9SO than for the other films because it is characteristic of the ester bonds from the triglyceride molecules (Velayutham, Abd-Majid, Ahmad, Kang, & Gan, 2009). The other peaks that were less important and common to all films are related to C=O stretching at 1697–1630 cm^{-1} (amide I) and N–H bending at 1545–1531 cm^{-1} (amide II). Finally, the band observed at 1336 cm^{-1} only in the FTIR spectrum of Q-8/CH/2.9SO corresponded to the CH_3 antisymmetric deformation of oleic acid in SO (Guerrero et al., 2011).

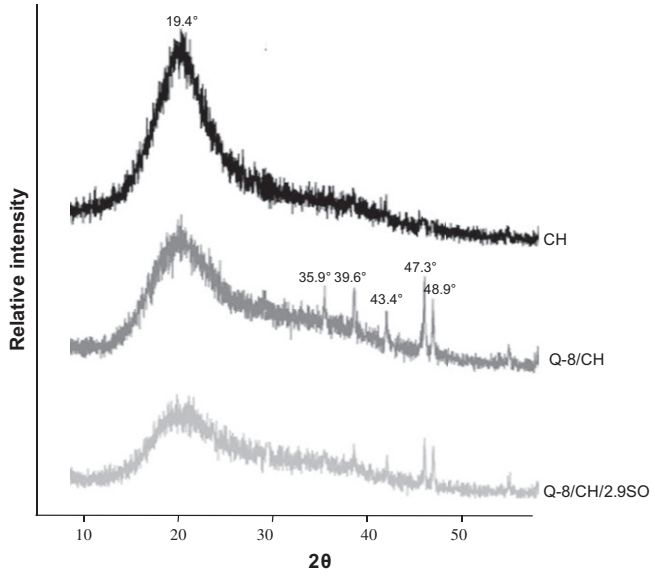

Fig. 2. X-ray diffraction profiles of chitosan film (CH), quinoa protein extract at pH 8/chitosan blend film (Q-8/CH) and quinoa protein extract at pH 8/chitosan/2.9 sunflower oil blend film (Q-8/CH/2.9SO).

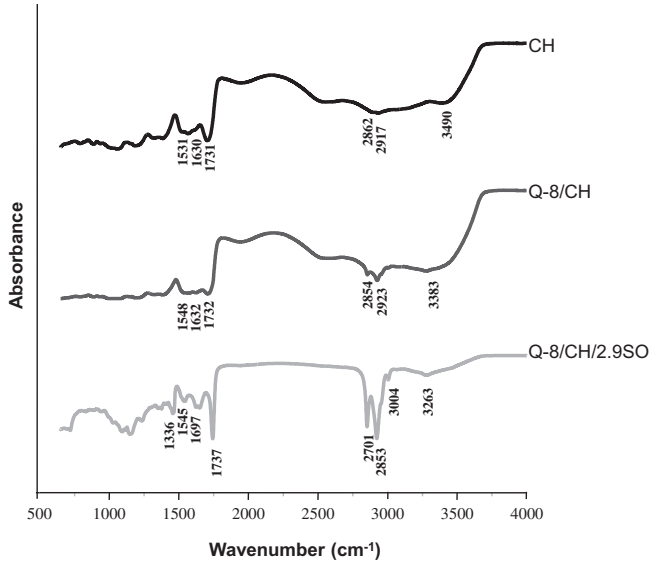

Fig. 3. FTIR spectra of chitosan film (CH), quinoa protein extract at pH 8/chitosan blend film (Q-8/CH) and quinoa protein extract at pH 8/chitosan/2.9 sunflower oil blend film (Q-8/CH/2.9SO).

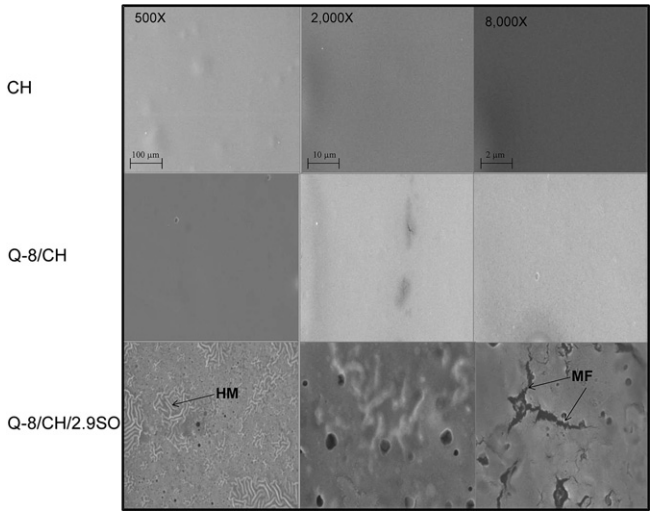

Fig. 4. SEM micrographs of the surface of chitosan film (CH), quinoa protein extract at pH 8/chitosan blend film (Q-8/CH) and quinoa protein extract at pH 8/chitosan/2.9 sunflower oil blend film (Q-8/CH/2.9SO). HM, hydrophobic mass. MF, microfractures.

3.3.3. Characterisation of film microstructure by SEM

Micrographs of the films are shown in Fig. 4. The SEM shows that the superficial structure of the CH and Q-8/CH blend films was homogeneous, continuous, compact and without pores. The micrographs clearly show the surfaces at different magnifications. The images suggest that the presence of quinoa protein does not generate discontinuities or porous structures when it is blended with CH, as reported by Abugoch et al. (2011).

However, a different superficial arrangement was observed after the incorporation of SO into the Q-8/CH/2.9SO blend film, which showed heterogeneous and rougher surfaces, with discontinuities associated with the formation of two phases (lipid globules and hydrocolloids) in the matrix (Vargas et al., 2009); these were observed as lipid droplets concentrated into hydrophobic masses (denoted as HM, Fig. 4) embedded in a continuous polymer phase composed of CH and Q-8, disrupting the matrix, increasing the film's heterogeneity and giving the surface of the material a rougher and more irregular character (Jiménez, Fabra, Talens, & Chiralt, 2012). This may be associated with the molecular aggregation of lipid molecules during the drying period of the film, contributing to the reduction in the WVP (Fabra et al., 2011; Phan The et al., 2009). The Q-8/CH/2.9SO blend film also showed micro-cracking matrices (denoted as MC, Fig. 4) and micropores of different shapes and sizes. The micro-cracking could be explained by the lower TS, and the micropores could be explained by the higher OP of this film (Park, Testin, Vergano, Park, & Weller, 1996).

3.4. Physicochemical properties

Table 2 shows the effects of incorporating quinoa protein and SO on the physicochemical properties of the CH film. Regarding the incorporation of quinoa protein and SO into the blend films, some differences in the a_w values were detected. The a_w values of the CH film were higher than those obtained for the Q-8/CH and Q-8/CH/2.9SO films, indicating that the free-water content was lower in this film due to the ionic interaction observed by FTIR.

With respect colour, the Q-8/CH and CH films were transparent, while the Q-8/CH blend film had a yellowish colour and the Q-8/CH/2.9SO blend film was opaque. This is because oil droplets of SO dispersed in the matrix affect the transparency; the interaction between SO and water molecules modifies the refractive index of hydrocolloid components, decreasing the transparency of the films (Pereda et al., 2012).

Table 2
Water activity (a_w) and colour parameters of chitosan film (CH), quinoa protein extract at pH 8/chitosan blend film (Q-8/CH) and quinoa protein extract at pH 8/chitosan/2.9 sunflower oil blend film (Q-8/CH/2.9SO).

Properties	Edible films		
	CH	Q-8/CH	Q-8/CH/2.9SO
a_w	0.58 ± 0.05^a	0.38 ± 0.04^b	0.29 ± 0.04^c
Colour	L^*: 15.1 ± 1.5^a	L^*: 17.2 ± 1.9^b	L^*: 51.0 ± 1.8^c
	a^*: -0.2 ± 0.1^a	a^*: -0.8 ± 0.2^b	a^*: 1.0 ± 0.2^c
	b^*: 0.2 ± 0.1^a	b^*: 1.7 ± 0.3^b	b^*: 20.1 ± 0.8^c
Chroma	0.3 ± 0.0^a	1.9 ± 0.2^b	20.1 ± 1.0^c
Hue angle	135 ± 15^a	115 ± 10^b	87 ± 5^c

Mean values in the same column with different superscripts differ significantly ($p < 0.05$).

4. Conclusions

Q-8/CH/SO blend films with improved WVP compared to Q-8/CH and CH films with different ratios of SO were obtained. Water-vapour permeation through the Q-8/CH/2.9SO composite films decreased compared to the WVP of the Q-8/CH and CH films owing to the non-polar nature of the lipids, which enhanced the hydrophobic interactions. Q-8/CH/2.9SO films were mechanically weaker than the Q-8/CH and CH films. The elongation at break increased from Q-8/CH and Q-8/CH/2.9SO due to the plasticising characteristics of the quinoa protein and lipid, in addition to the strong interactions developed between the lipid and hydrocolloid phases. The formation of the composite films in the absence of a plasticiser, producing good mechanical properties and lower WVP values, may lead to new applications in the food industry. The fields of application of Q/CH/SO blend on low pH fresh fruits, to increase shelf life and consumer acceptability.

References

Abugoch, L., Tapia, C., Villamán, M., Yazdani-Pedram, M., & Díaz-Dosque, M. (2011). Characterization of quinoa protein–chitosan blend edible films. *Food Hydrocolloids, 25*, 879–886.

Altenhofen, M., Krause, A., & Guenter, T. (2009). Alginate and pectin composite films crosslinked with Ca^{+2} ions: effect of the plasticizer concentration. *Carbohydrate Polymers, 77*(4), 736–742.

Andreuccetti, C., Carvalho, R., & Grosso, C. (2010). Gelatin-based films containing hydrophobic plasticizers and saponin from *Yucca schidigera* as the surfactant. *Food Research International, 43*(6), 1710–1718.

AOAC. (1996). *Official methods of analysis of AOAC International* (16th ed.). Gaithersburg, USA: AOAC International.

ASTM DIN 3935. (1981). *Standard test method for oxygen gas transmission rate through plastic films and sheeting using coulometric sensor.* USA: ASTM Book of Standards.

Bertan, L., Fakhouri, F., Siani, A., & Grosso, C. (2005). Influence of the addition of lauric acid to films made from gelatin, triacetin and a blend of stearic and palmitic acids. *Macromolecular Symposia, 229*, 143–149.

Bertan, L., Tanada-Palmu, P., Siani, A., & Grosso, C. (2005). Effect of fatty acids and 'Brazilian elemi' on composite films based on gelatin. *Food Hydrocolloids, 19*, 73–82.

Bonilla, J., Atarés, L., Vargas, M., & Chiralt, A. (2012). Effect of essential oils and homogenization conditions on properties of chitosan-based films. *Food Hydrocolloids, 26*, 9–16.

Bradford, M. (1976). Rapid and sensitive method for the quantization of micrograms quantities of protein utilizing the principle of protein dye binding. *Analytical Biochemistry, 72*, 248–254.

Cheng, L., Abd Karim, & Seow. (2008). Characterization of composite films made of konjac glucomannan (KGM), carboxymethyl cellulose (CMC) and lipid. *Food Chemistry, 107*, 411–418.

Fabra, M., Pérez-Masiá, R., Talens, P., & Chiralt, A. (2011). Influence of the homogenization conditions and lipid self-association on properties of sodium caseinate based films containing oleic and stearic acids. *Food Hydrocolloids, 25*, 1112–1121.

Falguera, V., Quintero, J., Jiménez, A., Muñoz, J., & Ibarz, A. (2011). Edible films and coatings: structures, active functions and trends in their use. *Trends in Food Science & Technology, 22*(6), 292–303.

García, M., Martino, M., & Zaritzky, N. (2000). Lipid addition to improve barrier properties of edible starch-based films and coatings. *Journal of Food Science, 65*(6), 941–947.

Ghanbarzadeh, B., & Almasi, H. (2011). Physical properties of edible emulsified films based on carboxymethyl cellulose and oleic acid. *International Journal of Biological Macromolecules, 48*, 44–49.

Ghasemlou, M., Khodaiyan, F., Oromiehie, A., & Saeid-Yarmand, M. (2011). Characterization of edible emulsified films with low affinity to water based on kefiran and oleic acid. *International Journal of Biological Macromolecules, 49*(3), 378–384.

Guerrero, P., Hanani, Z., Kerry, J., & Caba, K. (2011). Characterization of soy protein-based films prepared with acids and oils by compression. *Journal of Food Engineering, 107*, 41–49.

Ham-Pichavant, F., Sèbe, G., Pardon, P., & Coma, V. (2005). Fat resistance properties of chitosan-based paper packaging for food applications. *Carbohydrate Polymers, 61*(3), 259–265.

Jiménez, A., Fabra, M., Talens, P., & Chiralt, A. (2012). Effect of re-crystallization on tensile, optical and water vapour barrier properties of corn starch films containing fatty acids. *Food Hydrocolloids, 26*, 302–310.

Kester, J., & Fennema, O. (1989). Resistance of lipid films to oxygen transmission. *Journal of the American Oil Chemists' Society, 66*(8), 1129–1138.

Khwaldia, K., Banon, S., Desobry, S., & Hardy, J. (2004). Mechanical and barrier properties of sodium caseinate–anhydrous milk fat edible films. *International Journal of Food Science and Technology, 39*(4), 403–411.

Kowalczyk, D., & Baraniak, B. (2011). Effects of plasticizers, pH and heating of film forming solution on the properties of pea protein isolate films. *Journal of Food Engineering, 105*, 295–305.

Krochta, J. (2002). Proteins as raw materials for films and coatings: definitions, current status, and opportunities. In A. Gennadios (Ed.), *Protein based films and coatings* (pp. 1–41). Boca Raton, FL: CRC Press.

Kumar, R., Muzzarelli, R., Muzzarelli, C., Sashiwa, H., & Domb, A. (2004). Chitosan chemistry and pharmaceutical perspectives. *Chemical Reviews, 104*, 6017–6084.

McHugh, T., Aujard, J., & Krochta, J. (1994). Plasticized whey protein edible films: water vapor permeability properties. *Journal of Food Science, 59*(2), 416–419.

McHugh, T., & Krochta, J. (1994). Permeability properties of edible films. In J. M. Krochta, E. A. Baldwin, & M. O. Nisperos-Carriedo (Eds.), *Edible coatings and films to improve food quality* (pp. 139–187). Lancaster: Technomic Publishing Co., Inc.

Monedero, F., Fabra, M., Talens, T., & Chiralt, A. (2009). Effect of oleic acid–beeswax mixtures on mechanical, optical and water barrier properties of soy protein isolate based films. *Journal of Food Engineering, 91*, 509–515.

Morillon, V., Debeaufort, F., Blond, G., Capelle, M., & Voilley, A. (2002). Factors affecting the moisture permeability of lipid-based edible films: a review. *Critical Reviews in Food Science and Nutrition, 42*(1), 67–89.

Muik, B., Lendl, B., Molina-Díaz, A., & Ayora-Cañada, M. (2005). Direct monitoring of lipid oxidation in edible oils by Fourier transform Raman spectroscopy. *Chemistry and Physics of Lipids, 134*, 173–182.

Muzzarelli, R., Frega, N., Miliani, M., Muzzarelli, C., & Cartolari, M. (2000). Interactions of chitin, chitosan, N-lauryl chitosan and N-dimethylaminopropyl chitosan with olive oil. *Carbohydrate Polymers, 43*(3), 263–268.

NCh1151.Of76. (1999). *Norma Chilena Oficial: Láminas y películas plásticas – Determinación de las propiedades de tracción* (13 pp.).

NCh2098.Of2000. (2000). *Norma Chilena Oficial: Películas de recubrimiento orgánico–Determinación de la transmisión de vapor de agua* (13 pp.).

Nisperos-Carriedo, M. (1994). Edible coatings and films based on polysaccharides. In J. Krochta, E. Baldwin, & M. Nisperos-Carriedo (Eds.), *Protein-based films and coatings* (pp. 305–335). Lancaster: Technomic Publishing Co., Inc.

Park, J., Testin, R., Vergano, P., Park, H., & Weller, C. (1996). Fatty acid distribution and its effect on oxygen permeability in laminated edible films. *Journal of Food Science, 61*(2), 401–406.

Park, S., Marsh, K., & Rhim, J. (2002). Characteristics of different molecular weight chitosan films affected by the type of organic solvents. *Journal of Food Science, 67*(1), 194–197.

Péaroval, C., Debeaufort, F., Despera, D., & Voilley, A. (2002). Edible arabinoxylan-based films. 1. Effects of lipid type on water vapor permeability, film structure, and other physical characteristics. *Journal of Agricultural and Food Chemistry, 50*, 3977–3983.

Pereda, M., Amica, G., & Marcovich, N. (2012). Development and characterization of edible chitosan/olive oil emulsion films. *Carbohydrate Polymers, 87*(2), 1318–1325.

Pereda, M., Aranguren, M., & Marcovich, N. (2010). Caseinate films modified with tung oil. *Food Hydrocolloids, 24*, 800–808.

Perez-Gago, M., & Krochta, J. (2001). Lipid particle size effect on water vapor permeability and mechanical properties of whey protein/beeswax emulsion films. *Journal of Agricultural and Food Chemistry, 49*, 996–1002.

Perez-Gago, M., Rojas, C., & Del Rio, M. (2002). Effect of lipid type and amount of edible hydroxypropyl methylcellulose–lipid composite coatings used to protect postharvest quality of mandarins cv. fortune. *Journal of Food Science, 67*(8), 2903–2910.

Petersson, M., & Stading, M. (2005). Water vapour permeability and mechanical properties of mixed starch-monoglyceride films an effect on film forming conditions. *Food Hydrocolloids, 19*, 123–132.

Phan The, D., Debeaufort, F., Voilley, A., & Luu, D. (2009). Influence of hydrocolloid nature on the structure and functional properties of emulsified edible films. *Food Hydrocolloids, 23*, 691–699.

Prior, B. (1979). Measurement of water activity in foods: a review. *Journal of Food Protein, 42*, 668–674.

Sebti, I., Chollet, E., Degraeve, P., Noel, C., & Peyrol, E. (2007). Water sensitivity, antimicrobial, and physicochemical analyses of edible films based on HPMC and/or chitosan. *Journal of Agricultural and Food Chemistry, 55*, 693–699.

Shellhammer, T., & Krochta, J. (1997). Whey protein emulsion film performance as affected by lipid type and amount. *Journal of Food Science, 62*(2), 390–394.

Srinivasa, P., Rameshb, M., & Tharanathana, M. (2007). Effect of plasticizers and fatty acids on mechanical and permeability characteristics of chitosan films. *Food Hydrocolloids, 21*, 1113–1122.

Tanada-Palmu, P., & Grosso, C. (2005). Effect of edible wheat gluten-based films and coatings on refrigerated strawberry (*Fragaria × ananassa*) quality. *Postharvest Biology & Technology, 36*, 199–208.

Tapia, C., Costa, E., Moris, M., Sapag-Hagar, J., Valenzuela, F., & Basualto, C. (2002). Study of the influence of the pH media dissolution, degree of polymerization, and degree of swelling of the polymers on the mechanism of release of diltiazem from matrices based on mixtures of chitosan/alginate. *Drug Development and Industrial Pharmacy, 28*(2), 217–224.

Vargas, M., Albors, A., Chiralt, A., & González, C. (2009). Characterization of chitosan–oleic acid composite films. *Food Hydrocolloids, 23*, 536–547.

Velayutham, T., Abd-Majid, W., Ahmad, A., Kang, G., & Gan, S. (2009). Synthesis and characterization of polyurethane coatings derived from polyols synthesized with glycerol, phthalic anhydride and oleic acid. *Progress in Organic Coatings, 66*, 367–371.

Wong, D., Gastineau, F., Gregorski, K., Tillin, S., & Pavlath, A. (1992). Chitosan–lipid films. Microstructure and surface energy. *Journal of Agricultural and Food Chemistry, 40*, 540–544.

Zahedi, Y., Ghanbarzadeh, B., & Sedaghat, N. (2010). Physical properties of edible emulsified films based on pistachio globulin protein and fatty acids. *Journal of Food Engineering, 100*, 102–108.

Zhong, Y., Songa, X., & Li, Y. (2011). Antimicrobial, physical and mechanical properties of kudzu starch–chitosan composite films as a function of acid solvent types. *Carbohydrate Polymers, 84*, 335–342.